Environmental Pollution 311 (2022) 119933

Contents lists available at ScienceDirect

Environmental Pollution

journal homepage: www.elsevier.com/locate/envpol

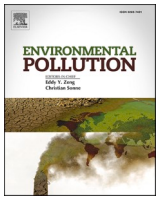

Systematic development of extraction methods for quantitative microplastics analysis in soils using metal-doped plastics☆

Alissa H. Tophinke [a,b], Akshay Joshi [b], Urs Baier [b], Rudolf Hufenus [c], Denise M. Mitrano [a,*]

[a] ETH Zurich, Department of Environmental Systems Science, Universitätstrasse 16, 8092, Zurich, Switzerland
[b] Zurich University of Applied Sciences, Life Sciences and Facility Management, Einsiedlerstrasse 31, 8820, Wädenswil, Switzerland
[c] Empa, Swiss Federal Laboratories for Materials Science and Technology, Lerchenfeldstrasse 5, 9014, St.Gallen, Switzerland

ARTICLE INFO

Keywords:
Microplastics
Soil
ICP-MS
Organic matter
CAZymes
Deep learning

ABSTRACT

The inconsistency of available methods and the lack of harmonization in current microplastics (MPs) analysis in soils demand approaches for extraction and quantification which can be utilized across a wide variety of soil types. To enable robust and accurate assessment of extraction workflows, PET MPs with an inorganic tracer (Indium, 0.2% wt) were spiked into individual soil subgroups and standard soils with varying compositions. Due to the selectivity of the metal tracer, MPs recovery rates could be quickly and quantitatively assessed using ICP-MS. The evaluation of different methods specifically adapted to the soil properties were assessed by isolating MPs from complex soil matrices by systematically investigating specific subgroups (sand, silt, clay, non-lignified and lignified organic matter) before applying the workflow to standard soils. Removal of recalcitrant organic matter is one of the major hurdles in isolating MPs for further size and chemical characterization, requiring novel approaches to remove lignocellulosic structures. Therefore, a new biotechnological method (3-F-Ultra) was developed which mimics natural degradation processes occurring in aerobic (Fenton) and anaerobic fungi (CAZymes). Finally, a Nile Red staining protocol was developed to evaluate the suitability of the workflow for non-metal-doped MPs, which requires a filter with minimal background residues for further chemical identification, e.g. by μFTIR spectroscopy. Image analysis was performed using a Deep Learning tool, allowing for discrimination between the number of residues in bright-field and MPs counted in fluorescence mode to calculate a Filter Clearness Index (FCI). To validate the workflow, three well-characterized standard soils were analyzed applying the final method, with recoveries of 88% for MPs fragments and 74% for MPs fibers with an average FCI of 0.75. Collectively, this workflow improves our current understanding of how to adapt extraction protocols according to the target soil composition, allowing for improved MPs analysis in environmental sampling campaigns.

1. Introduction

Although impacts of microplastics (MPs) in terrestrial environments are not completely understood, monitoring for the presence of MPs is of high importance to assess the current burden of MPs in the environment and track how concentrations change over time. The input of MPs into soils have been estimated to be 40 times greater than in freshwater bodies (Kawecki and Nowack, 2020), mostly because there is a large load coming from compost and sludge application onto land, mulching plastics, littering, street runoff and atmospheric deposition (Bläsing and Amelung, 2018). Understanding environmental exposure is important to link MPs accumulation to biological hazards (Campanale et al., 2020; Rillig et al., 2017; Selonen et al., 2020), thus enabling a more complete risk assessment (Mitrano and Wohlleben, 2020). Eventually, the goal would be to establish targeted legislative measures to limit MPs in soils. This is especially important in instances where direct additions may occur, such as recycled fertilizer applications.

Current sample and methodological biases make it inherently difficult to directly compare data on the occurrence of MPs in soils obtained with different protocols. Implicit to accurately quantifying MPs exposures in terms of MPs number, size and chemical composition is the establishment of harmonized extraction and characterization protocols

☆ This paper has been recommended for acceptance by Eddy Y. Zeng.

* Corresponding author.
E-mail address: denise.mitrano@usys.ethz.ch (D.M. Mitrano).

https://doi.org/10.1016/j.envpol.2022.119933
Received 8 June 2022; Received in revised form 22 July 2022; Accepted 6 August 2022
Available online 12 August 2022

to prevent under or overestimations of MPs concentrations in a given sample. A plethora of approaches have been suggested for the extraction of MPs from soils (Fuller and Gautam, 2016; Grbic et al., 2019; Han et al., 2019; Löder et al., 2017; Scopetani et al., 2020), where the workflow typically follows the procedure of 1) sample collection, 2) MPs extraction and 3) detection and chemical identification. For the latter step, microscopy Fourier-transform infrared microspectroscopy (μ-FTIR) or Raman microspectroscopy (μ-Raman) are used to simultaneously gain information about particle number, size, and chemical composition. These techniques are promising because they are non-destructive and the measurements can be automated in an analysis pipeline (Primpke et al., 2020; Primpke et al., 2017; Primpke et al., 2018). With the establishment of open-source spectral databases, such as siMPle (Primpke et al., 2018) or Open Specy (Cowger et al., 2020), it is expected that increasingly accurate spectral data will be available in the future. Nevertheless, these chemical imaging approaches require a filter free from non-target particles (e.g. sand, organics, etc.) as overlays may occur and which interfere with proper analysis (Löder et al., 2017). Consequently, extraction steps are essential for further spectroscopic detection methods.

At the outset of monitoring environmental concentrations of MPs, research was focused on assessing aquatic environments while terrestrial compartments were comparatively neglected (Ruggero et al., 2020; Wu et al., 2019). Although current methods for both MPs extraction and characterization are not yet standardized, there have been a number of inter-laboratory studies to assess the suitability of these techniques, particularly in water samples (Müller et al., 2020). Researchers have attempted to adopt extraction methods for measuring MPs in aqueous samples to be applied to soil samples, but the complex nature of soils are often overlooked (Thomas et al., 2020). Soils pose a significant challenge for MPs extraction because it is a heterogeneous mixture of inorganic and organic compounds, the compositions of these different components can vary widely (Da Costa et al., 2018), and the soil characteristics may influence the extraction efficiency (Radford et al., 2021). Therefore, in this study, the focus was explicitly placed on validating targeted extraction methods by systematically investigating single preselected soil subgroups (sand, silt, clay, non-lignified and lignified organic matter) to establish extraction chains for multi-component standard soils.

For the elimination of inorganic compounds, different approaches have been described in literature. Density and lipophilic separation can remove sand and silt, and subsequent filtration through stainless-steel filters can remove clay. The density of the flotation solution can be enhanced with different salts to separate denser mineral particles from less-dense MPs (Han et al., 2017). Lipophilic separation is another commonly used approach (Crichton et al., 2017; Mani et al., 2019; Scopetani et al., 2020), where the non-polar lipophilic component of the fatty acids in oils enable a bond with the non-polar lipophilic carbohydrate surface of synthetic polymer fragments (Mani et al., 2019). Soils with high organic contents pose the greatest challenge for isolating MPs and studies have reported that organic matter (OM) remaining on the MPs and/or filter after extraction can hinder proper chemical imaging and polymer identification when MPs are analyzed by spectroscopic techniques (Löder et al., 2017; Möller et al., 2021). Various approaches have been suggested, such as treatment with acid (Dehaut et al., 2016) or alkali (Hurley et al., 2018), oxidants (Nuelle et al., 2014) or enzymes (Löder et al., 2017), but they are either too strong and subsequently damage the polymers (Scheurer and Bigalke, 2018) or insufficiently remove OM, leaving OM residues on the MPs or filters which hinders subsequent chemical identification (Löder et al., 2017).

Certain fungi are known to degrade lignocellulose and thus the concept of mimicking natural degradation processes in the context of removing OM during MPs extraction and purification steps is promising. Lignin is difficult to chemically degrade due to the chemical complexity of its core structures. The biosynthesis is based on radical reactions of phenolic cinnamyl alcohols, resulting in a natural polymer that is arbitrarily linked and can therefore not be hydrolyzed (Kubicek, 2012). White rot fungi (WRF) have an oxidative ligninolytic system with various peroxidases, yet also include non-enzymatic mechanisms (Call and Mücke, 1997). Fenton-reaction is one of the non-enzymatic degradation processes appearing in WRF. Radicals produced by Fenton cause a series of cleavages by non-specifically attacking polysaccharides and lignin. This facilitates the enzymes to penetrate cell walls. In addition to aerobic fungi, anaerobic fungi have been found to be able to degrade plant biomass in the gastrointestinal tract of ruminants (Dollhofer et al., 2015). They colonize OM, such as straw fibers, and penetrate their surface thanks to rhizoidal growth and can subsequently degrade plant carbohydrates through a variety of carbohydrate-active enzymes (CAZymes) (Gruninger et al., 2018). CAZymes transcribed in sequenced anaerobic fungal isolates include different kinds of cellulases, hemicellulases, carbohydrate esterases, pectin lyase, pectin esterase and other enzymes (Gruninger et al., 2018). These cellulolytic enzymes can degrade the major hemicellulose components of plant cell walls, but not lignin (Berg and McClaugherty, 2014). By combining both processes of non-enzymatic radical attack from Fenton (as in aerobic fungi) and the use of CAZymes from anaerobic fungi, we propose a new approach to degrade lignocellulose to better isolate MPs in soils during an extraction workflow.

The aim of this work was to 1) systematically establish suitable extraction methods for extracting MPs in individual soil subgroup components in order to identify bottlenecks and improve individual extraction steps, 2) enable quick and quantitative recovery measurements in terms of plastic mass by using metal-doped PET MPs fragments and MPs fibers to circumvent the need for using challenging and not yet standardized plastic detection methods by spectroscopic techniques during the development of the extraction protocol, thus avoiding transmissible errors in the MPs analysis chain, 3) maximize the elimination of natural particles and obtain a filter with minimal residues necessary for further examination of non-doped MPs with chemical imaging instruments (e.g. μFTIR-microscope) and 4) ensure that the polymers were not altered and can be chemically identified after the extraction procedure. This methodological approach provides a new perspective for the validation of extraction methods specifically targeting soil constituents, where individual steps can be easily substituted for optimization depending on the target soil composition.

2. Materials and methods

2.1. Model metal-doped MPs fragments and fibers

Polyethylene terephthalate (PET) fragments (125–250 μm) and fibers (Ø 30 μm, 0.5–2,0 mm length) with an inclusion of 0.2% w/w Indium were developed in house to assess the extraction workflow, where the metal was measured as a proxy for plastic using ICP-MS. In two steps, PET (#5997, density 1.4 g/cm^3, by Serge Ferrari Tersuisse AG, Switzerland) was melt-mixed with In_2O_3 nanoparticles (Nanographi, 16–68 nm diameter) in a co-rotating 36 L/D twin screw extruder (Collin Lab & Pilot Solutions GmbH, Germany). First, 5 wt% In_2O_3 was mixed with 95% PET, followed by a second compounding with 95% PET, resulting in a final elemental indium content of approximately 0.2 wt%. The extrusion temperature and output were 300 °C and 0.8 kg/h, respectively. The polymer was dried for 8 h at 140 °C before compounding. Then, the extruded polymer was quenched down to room temperature on a conveyor belt before being pelletized. Pellets were ground with a rotor mill Pulverisette 14 (Fritsch, Germany), using liquid nitrogen to cool the polymer. The resulting powder was sieved on a vibratory shaker (Retsch, Germany) with stacked stainless-steel sieves with pore sizes of 250 and 125 μm, and MPs fragments with diameters 125–250 μm were collected in-between. MPs fibers were produced as described in Frehland et al. (2020) (Frehland et al., 2020). Metal leaching from the plastics did not occur over the course of the extraction tests, ensuring that the metal was a conservative tracer to measure

microplastics during the extraction workflow but was easily recoverable during microwave acid digestion and ICP-MS analysis (see Fig. S2 and Section 2.4).

2.2. Model soil components and standard soils

For method development, representative materials of certain soil subgroups (sand, silt, clay, non-lignified OM, lignified OM) were selected covering a wide range of soil compositions and textures to assess MPs recovery either alone or in mixtures. Soil subgroups included sand (quartz, 0.1–0.6 mm), silt (quartz flour, <40 μm), clay (Montmorillonite, Sigma Aldrich), non-lignified OM (wheat starch, Sigma Aldrich), OM (wheat straw, dried, milled to 2 mm). Subgroup mixtures of all representative soil components mentioned above (A: 2250 mg sand +2250 mg silt + 500 mg clay, B: 2200 mg sand +2200 mg silt + 400 mg clay + 200 mg non-lignified OM, C: all subgroups (B + 30 mg lignified OM) were made to assess the recovery along the extraction chain.

For the examination of the method in real soils, three different standard soils (LUFA, Germany) were selected including 1) LUFA 2.1 sand (86% sand, 11% silt, 3% clay and ca. 0.71% OM of the total mass.), 2) LUFA 2.4 sandy loam (33% sand, 41% silt, 26% clay and 2.03% OM) and 3) LUFA 6S clayey loam (25% sand, 34% silt, 41% clay and 1.77% OM) according to USDA. All samples were dried at 40 °C and passed through a 2 mm sieve before spiked addition of MPs fragments and fibers. Recovery rates were determined from triplicate extractions. A 2-way ANOVA with interactions was performed in R Studio (Version RStudio, 2022.02.0) and the TukeyHSD test was done to assess whether groups differed from each other (significant differences $p < 0.05$). Spike additions of a PET concentration of 0.1% of soil dry weight was chosen due to Swiss Chemical Risk Reduction Ordinance (CHemRRV), which limit the number of foreign plastic substances in compost and digestate to 0.1% of the dry matter (VVEA, 2021).

2.3. Targeted MPs extraction procedures and assessment of extraction workflow in soils

The development of tailored methods for each soil subgroup was done systematically by testing each subgroup in sequence for MPs recovery rate and matrix removal efficiency. Each subgroup had a targeted extraction treatment including physical (for sand, silt, clay), chemical (for non-lignified and lignified OM), or biological (for lignified OM) treatments. Subsequently, these individual extraction protocols were linked together for a sequential extraction protocol for mixtures of soil subgroups or for standard soils. For this, 5 mg MPs (fragments or fibers) were spiked into 5 g soil and select extraction treatments were applied, where MPs recovery rates (triplicates) and the Filter Clearness Index (FCI, duplicates) were determined. Additionally, 5 mg MPs were suspended in water and the efficiency of the entire procedure without solids was assessed to identify loss of MPs through the multi-step protocol.

To assess the FCI, a staining protocol with Nile Red (Sigma Aldrich) for PET was developed, combining different approaches from the literature (Erni-Cassola et al., 2017; Konde et al., 2020; Lv et al., 2019) to achieve a strong affinity of staining only for MPs, so that the natural components do not fluoresce. Previous investigation has shown that the amount of solution applied is irrelevant for the particle pixel brightness (data not shown). Therefore, Nile Red (5 mg/L) dissolved in acetone was dropped directly onto MPs placed on top of a stainless-steel filter, which was then incubated in an oven at 75 °C for 30 min. The experimental design is depicted in Fig. 1.

2.3.1. Removal of inorganic fractions with density, lipophilic and size separation

For density and lipophilic separations, 250 mL separating funnels were used which were marked with a pen on the outside of the glass before extractions at 5 mL and 100 mL to expediate the procedure. NaBr ($\rho = 1.55$ g*cm^{-3}) was used due to its non-toxicity (Liu et al., 2019), its ability to be recycled and because it is less expensive than other solutions used for density separation such as Sodium polytungstate hydrate (SPH, ρ up to 2.25 g*cm^{-3}) (Bläsing and Amelung, 2018). Approximately 5 mL of NaBr solution (ca. 95 g/100 ml water, 25 °C or recycled solution) was put into the funnel prior to soil addition to avoid clogging. Dried soil subcomponents or soil samples (5 g) spiked with 5 mg metal-doped PET were added with the help of a glass funnel to the separatory funnel and the walls were rinsed with NaBr with a glass pipette. The separatory funnel was then filled with NaBr-solution up to the 100 mL mark and shaken manually for 1 min. The entire device was subsequently ultrasonicated for 2 min and the solution was allowed to settle for 10 min. The heavy fraction, which accumulated at the bottom of the funnel and contained inorganic particles and NaBr solution, was drained (but kept for reuse) until only 1–2 cm of liquid with the light-density fraction remained. In cases where particles blocked the separatory funnel outlet, a needle was used to release the clogged funnel to drain the liquid. Approximately 5 mL of fresh NaBr solution was added to the separatory funnel, where the process was repeated until no

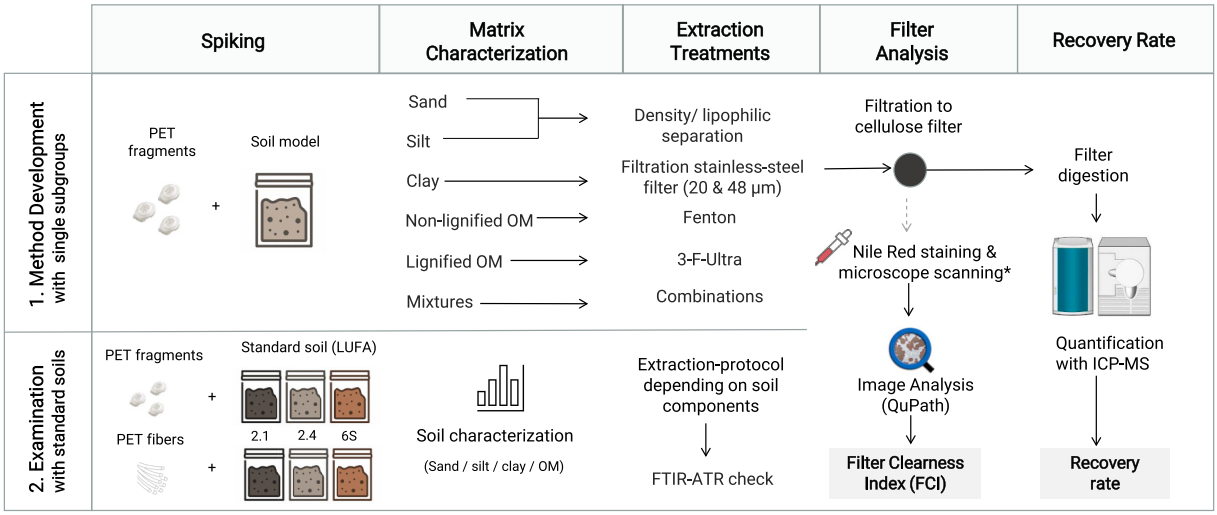

Fig. 1. Workflow of experimental design including 1. Method development with examination of 5 subgroups and mixtures and 2. Examination of the method with LUFA standard soils 2.1 (sand), 2.4 (loam), 6 S (clay). The recovery rate was calculated by measuring Indium as a proxy for the (metal-doped) MPs. *The FCI was assessed for the final extraction method with standard LUFA soils and PET particles.

dense particles were observed at the outlet of the separatory funnel. After separation was complete, the funnel was rinsed several times with Milli-Q water and the effluent was filtered through cellulose filters (MN-615, 55 mm, Macherey Nagel) with pore size of 4–12 μm to directly measure the samples for Indium content or through stainless-steel filters if further extraction steps are added.. At the end of each experiment, the remaining NaBr solution was collected and filtered through 11 μm cellulose filters to recycle the NaBr-solution. Before every new experimental replicate, solution density was controlled, where 1 mL of NaBr solution was weighted and if the density was below 1.50–1.55 g/mL, additional NaBr salt was added until the target density was reached. For the lipophilic extraction with oil, the same procedure was performed with the difference that a mix of 100 mL Milli-Q water and 10 mL rapeseed oil were used instead of NaBr solution.

For clay particles which remained in suspension during the density separation step, stainless steel filters with mesh sizes of 48 μm and 20 μm (custom-made, Rolf Körner GmbH, Germany) were used. The same stainless-steel filters were also used to combine different extraction steps, which was necessary for mixtures of the individual compounds and for the final protocol. Hereafter this step is called "backflushing", where the remaining MPs (and other residues) from one extraction step is washed back into the next vial with a spray bottle. To ensure minimal loss of MPs during filtration, a filter setup was used that securely holds the stainless-steel filter under vacuum, has no edges where the MPs could be lost and could be easily removed with tweezers (see Fig. S1, panel A).

2.3.2. Fenton's reaction for starch elimination as a representative component for non-lignified OM

Since various Fenton protocols have been recommended in literature (Al-Azzawi et al., 2020), the first step was to evaluate the success of wheat starch degradation without MPs by filtering the solution of starch and Fenton's reagent and weighing the dried cellulose filter after different Fenton reactions (all variant data not shown). The protocol which achieved a complete reduction in weight was selected for the final protocol, where 2 g of starch was spiked with 5 mg PET to evaluate MPs recovery rate during this step. The Fenton's reaction was performed in 250 mL beakers where spiked samples from weigh trays were transferred into the beaker with a spray bottle (maximum 5 mL Milli-Q water addition). A magnetic stirrer (lab disc, VWR) was used to continuously mix the solution. $FeSO_4 \cdot 7\ H_20$ (20 g/L) was adjusted to pH 3 with 2 M HNO_3 (approximately 10 drops/100 mL) and 5 mL of this solution was added to the beaker. To start the exothermic reaction, 5 mL of 30% H_20_2 (ROTIPURAN® p. a., ISO, stabilized, Carl Roth) was added after 2 min. The temperature was constantly monitored with a thermometer over the course of the 20 min degradation process and the vial was put into a water bath if the reaction temperature exceeded 60 °C. The solution was then ultrasonicated for 2 min, mixed with 200 mL Milli-Q water and filtered through a stainless-steel filter to remove excess iron.

2.3.3. Isolation and cultivation of anaerobic fungi Neocallimastix frontalis strain GBF20D4

The enzymes used to degrade lignocellulose were produced from the strain *Neocallimastix frontalis* GBF20D4 which were isolated from Chamois feces collected in the Alpine Forests in the Canton of Berne, Switzerland in February 2020 using the methodology described in Joshi et al. (2018) (Joshi et al., 2018). The medium used for isolation and enrichment was comprised of (per liter) 3 g yeast extract, 10 g tryptone, 150 ml of solution 1 (0.3% K_2HPO_4), 150 ml of solution 2 [0.3% KH_2PO_4, 0.6% $(NH_4)_2SO_4$, 0.6%NaCl, 0.06% $MgSO_4{\cdot}7H_2O$ and 0.06% $CaCl_2{\cdot}2H_2O$], 150 ml of depleted rumen fluid for enrichment (Leedle and Hespell, 1980) or distilled water for routine cultivation, 10 ml of trace element solution [0.025% $MnCl_2{\cdot}4H_2O$, 0.025% $NiCl_2{\cdot}6H_2O$, 0.0285 $Na_2MoO_4{\cdot}2H_2O$, 0.02% $FeSO_4{\cdot}7H_2O$, 0.005% $CoCl_2{\cdot}6H_2O$, 0.004% Na_2SeO_3, 0.003% $NaVO_3$, 0.0026% $ZnSO_4{\cdot}7H_2O$, 0.0021% $CuCO_4$], 1 ml resazurin (0.1%), 1 ml hemin (0.05%), 6 g $NaHCO_3$, 1 g L-cysteine-HCl, and 0.35 g of milled wheat straw (≈2 mm) as a carbon source in case of enrichment or 5 g of D-(+)-cellobiose for isolation. During the enrichment and isolation, 0.1% v/v penicillin G sodium salt, streptomycin sulphate, and ampicillin sodium salt (200 μg, 200 μg, and 100 μg/ml final concentration) were added to restrict bacterial growth. To ensure sufficient growth in the absence of rumen fluid in the minimal medium, 0.1% v/v cocktail of vitamin solution was added during the cultivation [0.001% Thiamine HCl, 0.02% Riboflavin, 0.06% Calcium pantothenate, 0.06% Niacin, 0.1% Nicotinamide, 0.005% Folic acid, 0.002% Cyanocobalamin, 0.02% Biotin, 0.01% Pyridoxamine, 0.01% p-Aminobenzoic acid]. In preliminary analysis, visual inspection and microscopic examinations were performed to study the morphological traits of the isolate. For molecular identification, the genomic DNA was extracted using the Plant/Fungi DNA Isolation kit (Sigma-Aldrich). The D1/D2 region of Large-Subunit (LSU) rDNA was amplified using NL1/NL4 primers (Edwards et al., 2017) and sequenced at Microsynth (Switzerland). The GenBank BLASTn was used to perform the sequences similarity search.

The morphological features and microscopic examination of the anaerobic fungi strain GBF20D4 (accession number ON386248) exhibited monocentric thallus and polyflagellated zoospores. Additionally, the BLAST search of obtained LSU sequences (700–750 bp) showed 99.54% similarity with *Neocallimastix frontalis* strain SR4 (accession number JN939158.1).

This strain GBF20D4 was sub-cultivated every week in 100 mL bottle containing 45 mL of medium and 350 mg wheat straw and incubated at 39 °C. Before sub-cultivation, pressure in the vials was measured as a quality check for successful growth, which should be approximately 1.2 bar ± 0.4. Then 0.5 mL vitamin solution was added to new media bottles. The enzyme solution was used after 5 days of growth, where 5 mL media including extracellular enzymes were removed using a sterile hypodermic needle (18G) and a 5 mL syringe under sterile conditions.

2.3.4. 3-F-Ultra method to degrade straw as a representative material for lignified OM

A new method (3-F-Ultra) was developed to reduce the most recalcitrant fraction in soil, i.e. lignocellulosic material including lignin. The method consisted of 1) Fenton-start (radical attack with reactive oxygen species (ROS)), 2) Fungal Enzymes (anaerobic fungi cultivation) and 3) Fenton-end (radical attack with ROS), and ultrasonication in between. To assess the method performance to degrade the model lignified OM, 30 mg of wheat straw (dried, milled to 2 mm) was incubated under different conditions (pH, temperature, incubation time), where degradation efficiency was measured by change in substate weight before and after treatment. Cellulase (TXL) shows its optimal reaction activity at pH 5.0 and 50 °C (Löder et al., 2017). Therefore, these conditions were also investigated. The pH was adjusted with nitric acid and pH was measured with pH-paper.

The protocol which achieved the most extensive degradation of straw by weight was used for the final protocol and straw was spiked with 5 mg PET to evaluate the recovery rate in this process step. Here, 30 mg straw and 5 mg MPs were transferred with 5 mL of Milli-Q water into a 250 mL beaker. The beaker was placed in an ultrasonic bath for 2 min and the material was subsequently exposed to reaction of Fenton-start (20 min reaction + 10 min cooling). The solution was then placed in an ultrasonic bath for 2 min. The liquid containing MPs was rinsed through a stainless-steel filter (20 μm pore size) and the vessel walls were rinsed thoroughly with Milli-Q water. The contents were poured into a 5 mL Petri dish, into which 5 mL of AF-solution (media + cultivated *Neocallimastix frontalis* GBF20D4 which produce extracellular fungal enzymes) were added with a syringe under sterile conditions. Glass petri dishes were wrapped with parafilm and incubated at 39 °C for 9 days, continuously shaken at 70 rpm. The contents were poured into a beaker using 5 mL of water to rinse, sonicated for 2 min, and then treated with Fenton-end (solution was kept overnight for further reaction with AF media, see section 3.2).

Furthermore, a test was conducted where the same method (3-F-Ultra) was applied to 30 mg wheat straw but incubated in water for 9 days instead of enzymes. Finally, the degradation rate of straw and the recovery rate of MPs for 2-F-Ultra was tested, where the first Fenton reaction was omitted.

2.4. Sample digestion and ICP-MS analysis to assess extraction workflow performance

After the extraction of each step (soil sub-components, mixtures, or model LUFA samples), MPs were collected on a cellulose filter (filtration setup shown in Figure S1 B) and the filter and MPs were directly digested in PTFE tubes (including 5 mL HNO_3 (65%)) with the Turbowave Simultaneous Automated Microwave Digestion System from MLS GmbH. The digestion program was as follows: 1) pressure was increased to 90 bar over the course of 20–30 min, 2) the temperature was ramped from 25 °C to 100 °C over the course of 8 min and held for 4 min at 100 °C, 3) the temperature was further increased to 200 °C over the course of 15 min and held at 200 °C for 30 min, 4) the pressure was released from the vessel and was cooled down to 25 °C. After sample digestion, the PTFE tubes were quantitatively rinsed with Milli-Q H_20 into a polypropylene Falcon tube and diluted to 50 mL (1:10). A further sample dilution of 1:50 was performed to achieve suitable metal concentrations for subsequent ICP-MS analysis.

The Indium dopant in the MPs was measured with Inductively Coupled Plasma - Mass Spectrometry (ICP-MS 7900, Agilent Technologies) featuring a coupled autosampler system (Agilent, SPS 4), micro-MIST Nebulizer and nickel cones. All instrument parameters were automatically tuned at the start of each day of analysis. An Indium standard solution of 100 μg/L was prepared daily for final dilutions of 0, 0.1, 0.5, 1, 2.5, 5, 12.5 and 25 ppb for instrument calibration. Rhodium (10 μg/1) was used as an internal standard across all measurements.

2.5. Quality assurance and quality controls (QA/QC)

To verify the accuracy of the measurement of Indium with ICP-MS, the LUFA soils and filters were measured for possible Indium background. Additionally, the linear relationship between the MPs weight and the Indium concentration was checked to ensure that the Indium concentration was evenly distributed in the metal-doped PET fragments and fibers. For this purpose, 2.5 mg, 5 mg, 10 mg PET MPs (in triplicates) were weighed, digested and the Indium concentrations were analyzed by ICP-MS (Fig. S2).

2.6. Extraction workflow selectivity for microplastics: image analysis and Filter Clearness Index (FCI)

To evaluate the clearness of the filter after developing the final extraction protocol, images of the filter were captured with a Leica Stereomicroscope M205 in both brightfield (BF) and fluorescence light (FL) (metadata in supplementary information). The fully motorized fluorescence stereomicroscope collected an image of the entire filter (55 mm diameter), by scanning multiple mosaic images and merging them together (metadata in Table S2). To achieve higher contrast between the filter and particulate matter, cellulose filters were dyed with black textile color (Rayher), where filters were sprayed and dried at 120 °C for 10 min and subsequently rinsed with water on both sides before use. After the solution was filtered through the black cellulose filter, the particles on it were fixed with a spray glue (Pattex, GlueSpray diluted in H_20) to minimize loss during transport and scanning with the microscope.

To count particles in both bright field and fluorescence light, a pre-trained Deep Learning approach (StarDist (Schmidt et al., 2018)) was applied, which was able to detect particles and count them automatically. StarDist, is a deep-learning-based method for 2D and 3D nucleus detection which runs in the open-source program QuPath (Version 0.3.1) (Bankhead et al., 2017). The trained model (dsb2018_heavy_augment.pb) was downloaded from GitHub and the parameters were adjusted as shown in Table S2. The detection channel was set to red for FL and green for BF. This enabled the software to distinguish and count particles that were in proximity. To ensure the same efficiency with all images made from fluorescence light, the contrast of the RGB images were modified (Image → Adjust →Brightness/Contrast → contrast to 85) with ImageJ (Version 1.53f51). To evaluate the trained model, certain regions of a test filter which contained both natural and MPs particles were counted by eye and compared with the result from the model in BF and FL. For this purpose, 10 small squares (1.6 mm^2) and 10 large squares (10 mm^2) were randomly selected. To quantitatively assess the ratio of MPs to natural particles on the filter after extraction, the Filter Clearness Index (FCI) was calculated by dividing the number of MPs that could be distinguished from natural particles after using a fluorescent dye by the number of total particles in brightfield mode. The closer the FCI was to 1, the fewer residual particles from the extraction process were present, which would facilitate the subsequent quantification and characterization of MPs in environmental samples.

2.7. Assessment of chemical changes to MPs after extraction workflow with FTIR-ATR

To ensure plastics were not chemically altered throughout the extraction workflow, MPs were analyzed with FTIR-ATR (PerkinElmer Spectrum Version 10.03.09) before and after extraction. The spectra were recorded over the wavenumber range of 600–4000 cm^{-1} using a spectral resolution of 4 cm^{-1} with 20 scans (using MIR TGS detector and Diamond/ZnSe Crystal) (Jung et al., 2018). The ATR spectra were pre-processed online (smoothing, baseline correction, range selection) and identified with Open Specy v0.9.3 (Cowger et al., 2020) to ensure whether the identification of the spectra is still possible after the treatment by comparing the spectra with the reference library (issued by the Pearson's r value).

3. Results and discussion

Extraction methods were developed for individual soil subgroup models with the goals of maximum recovery rate of the MPs (section 3.1) and maximum matrix elimination (section 3.2) without altering the polymers (section 3.4). After the development of single extraction steps, extraction chains were applied to subgroup mixtures before applying them to three standard soils from LUFA with different soil textures and OM contents, where the final method was evaluated based on the recovery rate and the FCI (section 3.3).

3.1. Targeted extraction protocols successfully extract PET fragments from simple and complex soil mixtures

Recovery rates of MPs fragments and fibers quantified by Indium measurements with ICP-MS were >90% for all single subgroup components (Fig. 2A), except for the lipophilic separation with rapeseed oil, which was not used further. Combining extraction steps to develop an extraction chain for mixtures of soil subgroups (Fig. 2B) also lead to recovery rates of >90%. Fig. 3 schematically shows the final extraction protocol for soils including all subgroups. This final protocol using density separation, filtration and 3-F-Ultra was also used for MPs spiked in water, resulting in a recovery rate of 92.7% ± 2.5, which indicates ca. 5–10% of fragments are lost solely from the number of MPs transfers along the extraction chain opposed to being entrapped in the matrix. It is hypothesized that backflushing filters may be the process step responsible for the highest loss throughout the procedure.

Radford et al. (2021) also reported that the characteristics of the soil medium is necessary to choose the optimal extraction method individually in soils (Radford et al., 2021). However, there the authors mixed soil with varying levels of sand, silt, clay and OM (as compost) together

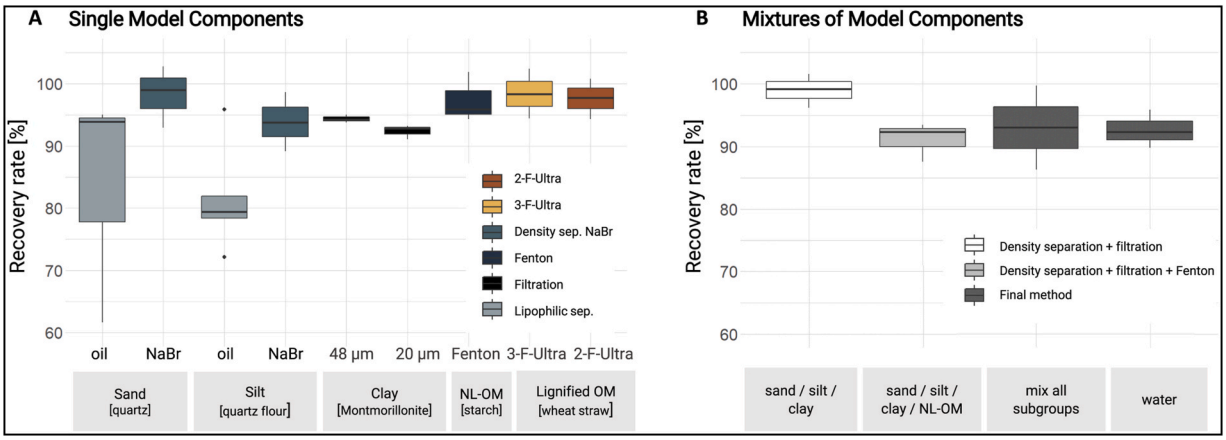

Fig. 2. A) Recovery rates evaluated from Indium measurements by ICP-MS for single model subgroup components (sand, silt, clay, non-lignified OM, lignified OM) in triplicate. The different colors represent the individual methods applied to the subgroup component. The Whisker plots show the median (crossed line), the 25–75% range in the box, the minimum and maximum values in the line and outliers as dots. B) Recovery rates of subgroup component mixtures by combining different methods (density separation + filtration for sand, silt, clay/density separation + filtration + Fenton for sand, silt, clay, non-lignified OM/density separation + filtration + 3-F-Ultra (final method, Fig. 3) for mixture of all subgroups and in water. (For interpretation of the references to color in this figure legend, the reader is referred to the Web version of this article.)

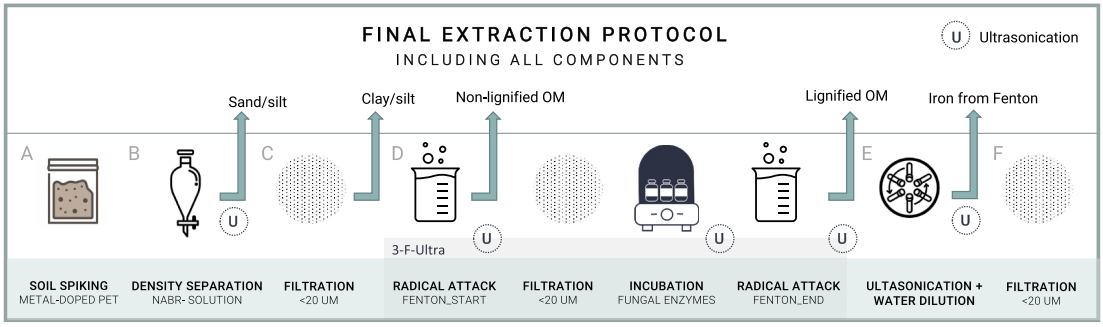

Fig. 3. Schematic overview of final method to isolate MPs from soil including all components (sand, silt, clay, OM). Nile red staining was afterwards directly carried out on the stainless-steel filters. (For interpretation of the references to color in this figure legend, the reader is referred to the Web version of this article.)

in bulk and did not investigate them individually beforehand. The approach used here has the advantage that the method can be broken down into its component parts and bottlenecks for each step can be identified and improved until 100% elimination of the matrix is achieved. By examining the properties of the soil a priori, a sample-specific extraction chain can be selected, where, e.g., the 3-F Ultra method can be omitted if small amount of OM is present in a sample (threshold to be determined).

3.2. 3-F-Ultra method significantly reduces OM content when extracting MPs from complex soil matrices

As current MPs extraction methods lack efficient approaches to sufficiently degrade OM, a focus was placed in this area. The development of the 3-F-Ultra (Fenton-start, incubation fungal enzymes, Fenton-end, ultrasonication in between) was conducted with 30 mg of wheat straw and the degradation efficiency was evaluated by weight loss. For the incubation step with extracellular enzymes, different growth conditions were examined where 9 days (39 °C, pH 7, no adjustment) lead to a 100% degradation of straw (i.e. complete liquidation of straw at the end of the incubation period). With shorter incubation times or when the pH was adjusted to 5, the straw was not completely degraded, including Fenton at the beginning and end and ultrasonication in between. Performing the same procedure (3-F-Ultra) without CAZymes in the media (H_20 instead) lead to a weight loss of only 55.5%, demonstrating that incubation with anaerobic fungi is essential for the degradation of straw.

Complete straw degradation was only possible when the AF-media was included in the Fenton-end reaction (when Fenton-end didn't include fungal media after incubation, the weight loss was only 59.7%). With the addition of the AF medium in Fenton-end, the pH remained neutral (as opposed to pH 3 as in the Fenton-start), and an increased reaction with gas formation was observed, and so consequently the Fenton-end was left overnight to completely react. Hemin, which is part of the AF cultivation media, may be responsible for this higher catalytic performance in straw degradation during Fenton-end. Hemin has received attention in the field of catalysis, due to its biologically active iron porphyrin molecule with peroxidase-like activity and high catalytic performance (Jiang et al., 2016). Hemin plays a key function in the redox processes of H_20_2 activation, has been used to mimic natural enzymes (Han et al., 2018) and consequently may be responsible for the complete degradation of straw in the final step of the 3-F-ultra method. However, the role of hemin in Fenton-end, as well in AF cultivation medium (Orpin and Greenwood, 1985) has not yet been clarified and further investigations were beyond the scope of this work.

Nevertheless, it could be shown that previous incubation with enzymes produced by the AF is essential, as Fenton-end with medium alone (without fungi) led only to a straw decomposition of 82.1%. After this investigation, the truncated method "2-F-Ultra", where the Fenton-start step was omitted, was examined showing a degradation of straw between 99 and 100% (n = 3). Therefore, in future studies, the 2-F Ultra method could be substituted for the elimination of straw, reducing processing steps and time. However, it must be noted that organic

matter is very light and even a high degradation of 99% still leaves visual residues on the filter, which may interfere with subsequent MPs detection using μFTIR.

According to Hurley et al. (2018) oxidation strategy utilizing Fenton reagent removed 80–87% of organics in sludge and 96–108% of organics in soil (Hurley et al., 2018). Nevertheless, Möller et al. (2021) used a similar protocol which did not lead to a complete removal of organic matter and thus hampered μ-FTIR measurements (Möller et al., 2021). Here the authors critiqued that total organic matter content was evaluated by loss-on-ignition (LOI), which is not an appropriate method in this instance, as inorganic material (e.g. $CaCO_3$) also can be oxidized and therefore lead to an overestimated reduction of OM. Instead, it was proposed to measure the reduction of OM on the filter by weight. By doing so, the authors reported an OM reduction of 77.2 ± 6.6%, with OM remaining on the filter. This study used nine steps in the final extraction method (density separation with $ZnCl_2$, SDS, Fenton, Protease, Pectinase, Viscozyme L, Cellulase, Fenton II, Density separation II) and achieved recovery rates of 92% (23/25 MPs) for PET fibers and fragments measured by μFTIR analysis. Löder et al. (2017) used a similar enzymatic purification method for surface water samples, however, this method also involved various individual enzyme steps with buffer changes, which is complex, time-consuming and required a total incubation period of up to 16 days (Löder et al., 2017). An overview of different methods developed for soil samples including a comparison of the recovery rate for PET and its limitations is shown in Table S3.

3.3. Evaluation of final method on standard soils by recovery rate and particle removal efficiency by FCI

To test the applicability of the final method for different soil textures, standard soils (LUFA 2.1, 2.4, 6S) were used to evaluate the recovery rate and the matrix removal efficiency determined by the FCI value. The mean recovery rate of MPs fragments (87.5 ± 7.7%) was higher than that of MPs fibers (73.7 ± 7.5%). Only LUFA 2.1 showed no significant difference between fibers and particles regarding recovery rate. For LUFA 2.4 and 6S, the recovery rate for fragments was higher than for fibers. It can therefore be shown that the probability of fibers being lost during this extraction chain is higher, potentially due to fibers being entrapped in the soil matrix during the density separation step or because of a larger likelihood of fibers flying away during backflushing. The overall mean FCI value was 0.75 for PET fragments, with a maximum value of 0.91 in LUFA 2.4. The result of the StarDist Model verification is shown in Fig. S3 and an example is given in Fig. S4. The pre-trained Deep Learning tool was easy to apply to our BF and FL images on black cellulose filters. The detection works for different particle sizes and morphologies on the filter in both modes. This Deep Learning tool in QuPath thus brings advantages that the investigation of particle removal efficiency can be performed faster, cheaper and on larger filters (55 mm diameter) than with μFTIR (typically 25 mm diameter). This can increase the efficiency of the filter examination in the method optimization phase, and, because of the high microscope resolution, visual inspection of the filters can give an impression of what kinds of residues remain on the filter.

The influence of soil texture on non-target (natural) particle removal and recovery rate was demonstrated with the LUFA 2.1 sample. LUFA 2.1 had the lowest MPs recovery rate (79%) as well as the lowest FCI (0.6) of all soils tested (Fig. 4). This soil contained mostly sand, which frequently clogged the opening of the separating funnel. This led to a suction effect when the sand particles were abruptly released with a needle, creating turbulation and thus probably causing the MPs to slide off with the inorganic fraction. Additionally, MPs may become stuck in the small opening. Furthermore, for this soil type, the inorganic fraction could not be completely eliminated even after multiple cleaning steps during density separation. This inability to sufficiently reduce the inorganic fraction during density separation was confirmed with visual inspection of the filters and quantified with the lower FCI. Therefore, it is worth considering whether larger separatory funnels or other glass vessels (e.g. as described in (Nakajima et al., 2019)) would result in higher recoveries and FCI for sandy soils, such as LUFA 2.1.

Monitoring MPs in soils to understand environmental exposure is an important task. While the method presented here is still time-consuming in terms of total number of days between the beginning and end of the experimental protocol, this is mainly because of the incubation period, which is a passive step without requiring active work from the researcher. Notably, compared to other extraction methods which used enzymes in an attempt to degrade organic matter, our one cocktail of enzymes from CAZymes does not necessitate incubation changes, thus reducing the active time required to manipulate samples and reduce the probability of losing MPs through extra vessel transfers. To further expedite the process, it is recommended to work with several samples in series (e.g. by using several separating funnels at the same time). Automation of the steps would be of great advantage but it is not yet feasible.

3.4. Extraction protocol does not impede correct polymer chemical identification

The evaluation of MPs fragments and fibers with FTIR-ATR before and after the complete extraction procedure indicate that the treatments do not hinder PET identification and thus do not alter the polymer chemistry after the extraction treatment. The spectra could be identified as PET after treatment with a Pearson's r coefficient of 0.96 for PET

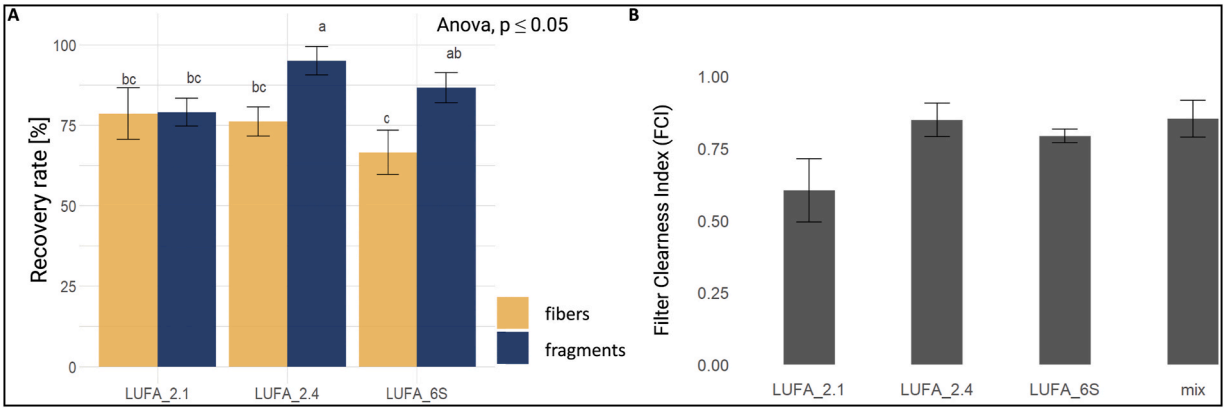

Fig. 4. A) Multiple comparison analysis of ANOVA and bar plots for recovery rates of PET particles LUFA 2.1 (n = 4) LUFA 2.4 (n = 5) LUFA 6 S (n = 4) and fibers (n = 3) in different LUFA standard soils. Different letters marked for bars represent significant differences ($p < 0.05$). B) Calculated FCI (n = 2) for MPs particles in different LUFA soils and soil model mixture including all components.

particles and 0.98 for PET fibers (Fig. S5). While it is not anticipated that the workflow would change the FTIR-ATR spectra of other plastics, this would need to be assessed on a case-by-case basis.

3.5. Further strategies and suggestions for method optimization

The modular design of the MPs extraction workflow presented here allows for the identification of bottlenecks and thus improvements can be done to individual steps in the method to improve recovery and FCI. These methods already show successful isolation of PET MPs from complex standard soils with recovery rates up to 100% and FCI up to 0.91 (LUFA 2.4), but still have the potential to be improved to reduce standard deviation in recovery rates and achieve equally high results for all soil types. For example, the elimination of inorganic matter should be improved to obtain a higher FCI for sandy soils. The small opening of the separatory funnels leads to blockages, and MPs could also be lost in the tight outlet. Therefore, instead of using separatory funnels for density separation, a glass separator as described in Nakajima et al. (2019) could help to avoid this issue in the future. NaBr solution can also be substituted by e.g. SPH, if polymers with higher densities have to be extracted.

The experiments performed here were only conducted with pristine PET fragments and fibers in limited size fractions. Since MPs in the environment consist of a wide variety of polymers, sizes and morphologies, additional model MPs, including weathered MPs, need to be investigated in further studies. Of particular importance would be to assess when MPs are embedded in soil aggregates, as this may influence extraction and recovery rates. For example, by dispersing soil aggregates with sodium hexametaphosphate before density separation, MPs trapped in or covered by soil aggregates could be liberated for more efficient extraction (Radford et al., 2021; Steinmetz et al., 2022). Furthermore, a FCI threshold could be set to evaluate the sufficiency of extraction for further measurements with non-doped MPs. This could be done with chemical imaging instruments (e.g. μFTIR-microscope) with connected fluorescent light. By attaching a LED with a specific wavelength to an FTIR device (for fluorescence of Nile Red, ca. 490 nm), the filters could be investigated after the here presented methods applied. To verify that only MPs were measured on the device without residues, a comparison between the result of the device and the Deep-Learning-Tool presented here can be performed. Therefore, it is also important to further investigate the applicability of the staining method to other polymer types. Nel et al. (2021) have also recommended polymer-specific staining (Nel et al., 2021). Since the staining is done on a stainless-steel filter, a multi-stage staining with different sequential Nile red solutions would be a possible suggestion that needs to be tested.

4. Conclusions

The use of a wide variety of MPs extraction methods in different studies creates associated biases and makes it difficult to directly compare data on the occurrence and quantification in terms of number or mass of MPs in soils. The aim of this work was to systematically validate individual method steps for single soil subgroups, as soil texture and contents may influence MPs extraction before chemical identification and size analysis. By using metal-doped MPs fragments and fibers, we were able to conduct a systematic study more easily, as we were able to measure smaller MPs in a larger number of samples since we avoided time-consuming processes such as μFTIR analysis. Recovery rates could be accurately quantified thanks to the metal-doped MPs, even for a high quantity of spiked MPs (0.1% of soil dry matter). Here, tailored methods for individual model subgroups were developed and successfully linked together to achieve high MPs recovery for both MPs fragments and MPs fibers (88% and 74% respectively in standard LUFA soils) with minimal natural residues remaining on the final sample filter. A particular advantage of this method was that a cocktail of enzymes was produced by cultivating anaerobic fungi, which were then incubated with the sample, so that no time-consuming buffer changes for single (costly) enzymes needed to be conducted as has been suggested in previous studies. Here, a nature-inspired solution was found using CAZymes to hydrolyze a range of different carbohydrates and achieve a Fenton reaction with higher catalytic activity to reduce OM. This eventually led to 100% degradation of high masses of lignin-containing straw (30 mg) with the application of the 3-F Ultra method. While the transferability of the extraction methods presented here should be assessed for other MPs polymers and plastics (including weathered MPs), we have shown that the characterization of soil texture and organic matter content may help in selecting the best extraction steps for a given soil type. The approach established here breaks down individual problems occurring in complex soil matrices into their component parts, allowing specific optimizations to be made and bottlenecks to be identified. These systematically developed methods thus open new perspectives for the analysis of MPs in soils and are a step towards future harmonization of MPs extraction protocols in heterogenous solid samples.

Author statement

Alissa H. Tophinke: Formal analysis, Investigation, Methodology, Writing – original draft, Writing – review & editing. Askay Joshi: Methodology, Writing – review & editing. Urs Baier: Supervision, Writing – review & editing. Rudolf Hufenus: Resources, Writing – review & editing. Denise M. Mitrano: Conceptualization, Funding acquisition, Project administration, Supervision, Writing – original draft, Writing – review and editing.

Funding sources

D.M.M. was funded through the Swiss National Science Foundation (grant number PCEFP2_186856).

Declaration of competing interest

The authors declare the following financial interests/personal relationships which may be considered as potential competing interests: Denise Mitrano reports financial support was provided by Swiss National Science Foundation.

Data availability

Data will be made available on request.

Acknowledgments

Nora Bernet conducted preliminary experiments to assess Indium concentration in the model microplastics and first trials for the lipophilic extraction protocols. Mathias Lienhard and Benno Wüst (EMPA, Switzerland) prepared the PET-In compounds and the MPs fragments, respectively.

Appendix A. Supplementary data

Supplementary data to this article can be found online at https://doi.org/10.1016/j.envpol.2022.119933.

References

Al-Azzawi, M.S.M., Kefer, S., Weißer, J., Reichel, J., Schwaller, C., Glas, K., Knoop, O., Drewes, J.E., 2020. Validation of sample preparation methods for microplastic analysis in wastewater matrices—reproducibility and standardization. Water 12, 2445. https://doi.org/10.3390/w12092445.

Bankhead, P., Loughrey, M.B., Fernández, J.A., Dombrowski, Y., McArt, D.G., Dunne, P. D., McQuaid, S., Gray, R.T., Murray, L.J., Coleman, H.G., James, J.A., Salto-Tellez, M., Hamilton, P.W., 2017. QuPath: open source software for digital pathology image analysis. Sci. Rep. 7, 16878. https://doi.org/10.1038/s41598-017-17204-5.

Berg, B., McClaugherty, C., 2014. Plant Litter. Decomposition, Humus Formation, Carbon Sequestration.
Bläsing, M., Amelung, W., 2018. Plastics in soil: analytical methods and possible sources. Sci. Total Environ. 612, 422–435. https://doi.org/10.1016/j.scitotenv.2017.08.086.
Call, H.P., Mücke, I., 1997. History, overview and applications of mediated lignolytic systems, especially laccase-mediator-systems (Lignozym®-process). J. Biotechnol. 53, 163–202. https://doi.org/10.1016/S0168-1656(97)01683-0.
Campanale, C., Massarelli, C., Savino, I., Locaputo, V., Uricchio, V.F., 2020. A detailed review study on potential effects of microplastics and additives of concern on human health. Int. J. Environ. Res. Publ. Health 17, 1212. https://doi.org/10.3390/ijerph17041212.
Cowger, W., Gray, A., Christiansen, S.H., DeFrond, H., Deshpande, A.D., Hemabessiere, L., Lee, E., Mill, L., Munno, K., Ossmann, B.E., Pittroff, M., Rochman, C., Sarau, G., Tarby, S., Primpke, S., 2020. Critical review of processing and classification techniques for images and spectra in microplastic research. Appl. Spectrosc. 74, 989–1010. https://doi.org/10.1177/0003702820929064.
Crichton, E.M., Noël, M., Gies, E.A., Ross, P.S., 2017. A novel, density-independent and FTIR-compatible approach for the rapid extraction of microplastics from aquatic sediments. Anal. Methods 9, 1419–1428. https://doi.org/10.1039/C6AY02733D.
Da Costa, J., Paço, A., Santos, P., Duarte, A., Rocha-Santos, T., 2018. Microplastics in soils: assessment, analytics and risks. Environ. Chem. 16 https://doi.org/10.1071/EN18150.
Dehaut, A., Cassone, A.-L., Frère, L., Hermabessiere, L., Himber, C., Rinnert, E., Rivière, G., Lambert, C., Soudant, P., Huvet, A., Duflos, G., Paul-Pont, I., 2016. Microplastics in seafood: benchmark protocol for their extraction and characterization. Environ. Pollut. 215, 223–233. https://doi.org/10.1016/j.envpol.2016.05.018.
Dollhofer, V., Podmirseg, S.M., Callaghan, T.M., Griffith, G.W., Fliegerová, K., 2015. Anaerobic fungi and their potential for biogas production. Adv. Biochem. Eng. Biotechnol. 151, 41–61. https://doi.org/10.1007/978-3-319-21993-6_2.
Edwards, J.E., Forster, R.J., Callaghan, T.M., Dollhofer, V., Dagar, S.S., Cheng, Y., Chang, J., Kittelmann, S., Fliegerova, K., Puniya, A.K., Henske, J.K., Gilmore, S.P., O'Malley, M.A., Griffith, G.W., Smidt, H., 2017. PCR and omics based techniques to study the diversity, ecology and biology of anaerobic fungi: insights, challenges and opportunities. Front. Microbiol. 8.
Erni-Cassola, G., Gibson, M.I., Thompson, R.C., Christie-Oleza, J.A., 2017. Lost, but found with nile red: a novel method for detecting and quantifying small microplastics (1 mm to 20 μm) in environmental samples. Environ. Sci. Technol. 51, 13641–13648. https://doi.org/10.1021/acs.est.7b04512.
Frehland, S., Kaegi, R., Hufenus, R., Mitrano, D.M., 2020. Long-term assessment of nanoplastic particle and microplastic fiber flux through a pilot wastewater treatment plant using metal-doped plastics. Water Res. 182, 115860. https://doi.org/10.1016/j.watres.2020.115860.
Fuller, S., Gautam, A., 2016. A procedure for measuring microplastics using pressurized fluid extraction. Environ. Sci. Technol. 50, 5774–5780. https://doi.org/10.1021/acs.est.6b00816.
Grbic, J., Nguyen, B., Guo, E., You, J.B., Sinton, D., Rochman, C.M., 2019. Magnetic extraction of microplastics from environmental samples. Environ. Sci. Technol. Lett. 6, 68–72. https://doi.org/10.1021/acs.estlett.8b00671.
Gruninger, R.J., Nguyen, T.T.M., Reid, I.D., Yanke, J.L., Wang, P., Abbott, D.W., Tsang, A., McAllister, T., 2018. Application of transcriptomics to compare the carbohydrate active enzymes that are expressed by diverse genera of anaerobic fungi to degrade plant cell wall carbohydrates. Front. Microbiol. 9, 1581. https://doi.org/10.3389/fmicb.2018.01581.
Han, X., Liu, W., Huang, J.-W., Ma, J., Zheng, Y., Ko, T.-P., Xu, L., Cheng, Y.-S., Chen, C.-C., Guo, R.-T., 2017. Structural insight into catalytic mechanism of PET hydrolase. Nat. Commun. 8, 2106. https://doi.org/10.1038/s41467-017-02255-z.
Han, X., Lu, X., Vogt, R.D., 2019. An optimized density-based approach for extracting microplastics from soil and sediment samples. Environ. Pollut. 254, 113009. https://doi.org/10.1016/j.envpol.2019.113009.
Han, Z., Li, J., Han, X., Zhao, X., Ji, X., 2018. A novel biomimetic catalyst constructed by axial coordination of hemin with PAN fiber for efficient degradation of organic dyes. J. Mater. Sci. 53, 1–14. https://doi.org/10.1007/s10853-017-1899-3.
Hurley, R.R., Lusher, A.L., Olsen, M., Nizzetto, L., 2018. Validation of a method for extracting microplastics from complex, organic-rich, environmental matrices. Environ. Sci. Technol. 52, 7409–7417. https://doi.org/10.1021/acs.est.8b01517.
Jiang, B., Yao, Y., Xie, R., Dai, D., Lu, W., Chen, W., Zhang, L., 2016. Enhanced generation of reactive oxygen species for efficient pollutant elimination catalyzed by hemin based on persistent free radicals. Appl. Catal. B Environ. 183, 291–297. https://doi.org/10.1016/j.apcatb.2015.10.051.
Joshi, A., Lanjekar, V.B., Dhakephalkar, P.K., Callaghan, T.M., Griffith, G.W., Dagar, S.S., 2018. Liebetanzomyces polymorphus gen. et sp. nov., a new anaerobic fungus (Neocallimastigomycota) isolated from the rumen of a goat. Manuf. Confect. (MC) 40, 89–110. https://doi.org/10.3897/mycokeys.40.28337.
Jung, M.R., Horgen, F.D., Orski, S.V., Rodriguez, C.V., Beers, K.L., Balazs, G.H., Jones, T. T., Work, T.M., Brignac, K.C., Royer, S.-J., Hyrenbach, K.D., Jensen, B.A., Lynch, J. M., 2018. Validation of ATR FT-IR to identify polymers of plastic marine debris, including those ingested by marine organisms. Mar. Pollut. Bull. 127, 704–716. https://doi.org/10.1016/j.marpolbul.2017.12.061.
Kawecki, D., Nowack, B., 2020. A proxy-based approach to predict spatially resolved emissions of macro- and microplastic to the environment. Sci. Total Environ. 748, 141137. https://doi.org/10.1016/j.scitotenv.2020.141137.
Konde, S., Ornik, J., Prume, J.A., Taiber, J., Koch, M., 2020. Exploring the potential of photoluminescence spectroscopy in combination with Nile Red staining for microplastic detection. Mar. Pollut. Bull. 159, 111475. https://doi.org/10.1016/j.marpolbul.2020.111475.
Kubicek, C.P., 2012. Fungi and Lignocellulosic Biomass. John Wiley & Sons.
Leedle, J.A., Hespell, R.B., 1980. Differential carbohydrate media and anaerobic replica plating techniques in delineating carbohydrate-utilizing subgroups in rumen bacterial populations. Appl. Environ. Microbiol. 39, 709–719. https://doi.org/10.1128/aem.39.4.709-719.1980.
Liu, M., Song, Y., Lu, S., Qiu, R., Hu, J., Li, X., Bigalke, M., Shi, H., He, D., 2019. A method for extracting soil microplastics through circulation of sodium bromide solutions. Sci. Total Environ. 691, 341–347. https://doi.org/10.1016/j.scitotenv.2019.07.144.
Löder, M.G.J., Imhof, H.K., Ladehoff, M., Löschel, L.A., Lorenz, C., Mintenig, S., Piehl, S., Primpke, S., Schrank, I., Laforsch, C., Gerdts, G., 2017. Enzymatic purification of microplastics in environmental samples. Environ. Sci. Technol. 51, 14283–14292. https://doi.org/10.1021/acs.est.7b03055.
Lv, L., Qu, J., Yu, Z., Chen, D., Zhou, C., Hong, P., Sun, S., Li, C., 2019. A simple method for detecting and quantifying microplastics utilizing fluorescent dyes - safranine T, fluorescein isophosphate, Nile red based on thermal expansion and contraction property. Environ. Pollut. 255, 113283. https://doi.org/10.1016/j.envpol.2019.113283.
Mani, T., Frehland, S., Kalberer, A., Burkhardt-Holm, P., 2019. Using castor oil to separate microplastics from four different environmental matrices. Anal. Methods 11, 1788–1794. https://doi.org/10.1039/C8AY02559B.
Mitrano, D.M., Wohlleben, W., 2020. Microplastic regulation should be more precise to incentivize both innovation and environmental safety. Nat. Commun. 11, 5324. https://doi.org/10.1038/s41467-020-19069-1.
Möller, J.N., Heisel, I., Satzger, A., Vizsolyi, E.C., Oster, S.D.J., Agarwal, S., Laforsch, C., Löder, M.G.J., 2021. Tackling the challenge of extracting microplastics from soils: a protocol to purify soil samples for spectroscopic analysis. Environ. Toxicol. Chem. https://doi.org/10.1002/etc.5024 n/a.
Müller, Y.K., Wernicke, T., Pittroff, M., Witzig, C.S., Storck, F.R., Klinger, J., Zumbülte, N., 2020. Microplastic analysis—are we measuring the same? Results on the first global comparative study for microplastic analysis in a water sample. Anal. Bioanal. Chem. 412, 555–560. https://doi.org/10.1007/s00216-019-02311-1.
Nakajima, R., Tsuchiya, M., Lindsay, D.J., Kitahashi, T., Fujikura, K., Fukushima, T., 2019. A new small device made of glass for separating microplastics from marine and freshwater sediments. PeerJ 7, e7915. https://doi.org/10.7717/peerj.7915.
Nel, H.A., Chetwynd, A.J., Kelleher, L., Lynch, I., Mansfield, I., Margenat, H., Onoja, S., Goldberg Oppenheimer, P., Sambrook Smith, G.H., Krause, S., 2021. Detection limits are central to improve reporting standards when using Nile red for microplastic quantification. Chemosphere 263, 127953. https://doi.org/10.1016/j.chemosphere.2020.127953.
Nuelle, M.-T., Dekiff, J.H., Remy, D., Fries, E., 2014. A new analytical approach for monitoring microplastics in marine sediments. Environ. Pollut. 184, 161–169. https://doi.org/10.1016/j.envpol.2013.07.027.
Orpin, C.G., Greenwood, Y., 1985. The role of haems and related compounds in the nutrition and zoosporogenesis of the rumen chytridiomycete neocallimastx frontalis H8. Microbiology 131, 2591–2594. https://doi.org/10.1099/00221287-132-8-2179.
Primpke, S., Godejohann, M., Gerdts, G., 2020. Rapid identification and quantification of microplastics in the environment by quantum cascade laser-based hyperspectral infrared chemical imaging. Environ. Sci. Technol. 54, 15893–15903. https://doi.org/10.1021/acs.est.0c05722.
Primpke, S., Lorenz, C., Rascher-Friesenhausen, R., Gerdts, G., 2017. An automated approach for microplastics analysis using focal plane array (FPA) FTIR microscopy and image analysis. Anal. Methods 9, 1499–1511. https://doi.org/10.1039/C6AY02476A.
Primpke, S., Wirth, M., Lorenz, C., Gerdts, G., 2018. Reference database design for the automated analysis of microplastic samples based on Fourier transform infrared (FTIR) spectroscopy. Anal. Bioanal. Chem. 410 https://doi.org/10.1007/s00216-018-1156-x.
Radford, F., Zapata-Restrepo, L.M., Horton, A.A., Hudson, M.D., Shaw, P.J., Williams, I. D., 2021. Developing a systematic method for extraction of microplastics in soils. Anal. Methods 13, 1695–1705. https://doi.org/10.1039/D0AY02086A.
Rillig, M.C., Ziersch, L., Hempel, S., 2017. Microplastic transport in soil by earthworms. Sci. Rep. 7, 1362. https://doi.org/10.1038/s41598-017-01594-7.
Ruggero, F., Gori, R., Lubello, C., 2020. Methodologies for microplastics recovery and identification in heterogeneous solid matrices: a review. J. Polym. Environ. 28, 739–748. https://doi.org/10.1007/s10924-019-01644-3.
Scheurer, M., Bigalke, M., 2018. Microplastics in Swiss floodplain soils. Environ. Sci. Technol. 52, 3591–3598. https://doi.org/10.1021/acs.est.7b06003.
Schmidt, U., Weigert, M., Broaddus, C., Myers, G., 2018. Cell Detection with Star-convex Polygons. arXiv:180603535 [cs], vol. 11071, pp. 265–273. https://doi.org/10.1007/978-3-030-00934-2_30.
Scopetani, C., Chelazzi, D., Mikola, J., Leiniö, V., Heikkinen, R., Cincinelli, A., Pellinen, J., 2020. Olive oil-based method for the extraction, quantification and identification of microplastics in soil and compost samples. Sci. Total Environ. 733, 139338. https://doi.org/10.1016/j.scitotenv.2020.139338.
Selonen, S., Dolar, A., Jemec Kokalj, A., Skalar, T., Parramon Dolcet, L., Hurley, R., van Gestel, C.A.M., 2020. Exploring the impacts of plastics in soil – the effects of polyester textile fibers on soil invertebrates. Sci. Total Environ. 700, 134451. https://doi.org/10.1016/j.scitotenv.2019.134451.
Steinmetz, Z., Löffler, P., Eichhöfer, S., David, J., Muñoz, K., Schaumann, G.E., 2022. Are agricultural plastic covers a source of plastic debris in soil? A first screening study. SOIL 8, 31–47. https://doi.org/10.5194/soil-8-31-2022.

Thomas, D., Schütze, B., Heinze, W.M., Steinmetz, Z., 2020. Sample preparation techniques for the analysis of microplastics in soil—a review. Sustainability 12, 9074. https://doi.org/10.3390/su12219074.

Vvea, 2021. SR 814.81 Verordnung vom 18. Mai 2005 zur Reduktion von Risiken beim Umgang mit bestimmten besonders gefährlichen Stoffen, Zubereitungen und Gegenständen (Chemikalien-Risikoreduktions-Verordnung, ChemRRV) - Version 01.01.2021.

Wu, P., Huang, J., Zheng, Y., Yang, Y., Zhang, Y., He, F., Chen, H., Quan, G., Yan, J., Li, T., Gao, B., 2019. Environmental occurrences, fate, and impacts of microplastics. Ecotoxicol. Environ. Saf. 184, 109612. https://doi.org/10.1016/j.ecoenv.2019.109612.